ACS OMEGA

Open Access

http://pubs.acs.org/journal/acsodf

Article

Experimental Study on the Explosion Parameters of *n*-Decane Aerosol under Saturated Vapor Pressure

Yue Wang, Xueling Liu, and Chang Qi*

Cite This: *ACS Omega* 2024, 9, 6381−6390

Read Online

ACCESS | Metrics & More | Article Recommendations

ABSTRACT: This research aims to conduct a comprehensive investigation and analysis of the effects of particle size and concentration on crucial explosion parameters in *n*-decane aerosols. Two sets of *n*-decane aerosols with different concentrations were initially measured, with Sauter mean diameters of 22 and 38 μm, respectively. These measurements served as the foundation for understanding the impact of the particle size on explosion parameters. Subsequently, experiments were performed on *n*-decane aerosols with various concentrations, utilizing an ignition energy of 40.32 J. The analysis focused on critical explosion parameters including the lower flammability limit, explosion pressure, explosion temperature, and flame propagation delay time. Through thorough examination of the data obtained from these experiments, the research elucidated the relationship between *n*-decane concentration, particle size, and these explosion parameters.

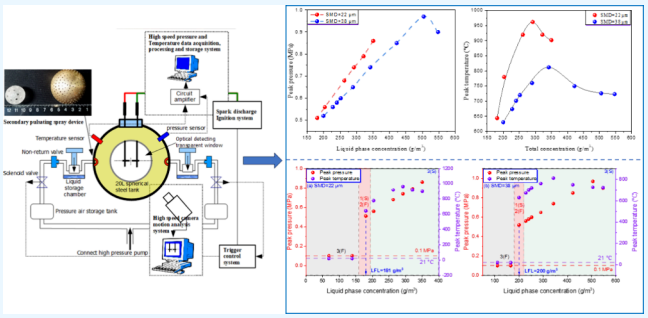

1. INTRODUCTION

There are well-established hazardous area classifications for explosive gas atmospheres, set out in numerous standards and industry codes of practice.[1] However, this is not the case for liquid releases with high flashpoints, which could produce an explosive aerosol atmosphere.[2−4] Mist explosion hazards are given qualitative guidance in a new annex to BS EN 60079-10-1,[5] but no quantitative methods are provided.[6] The Energy Institute Code of Practice IP15[7] emphasizes the need for additional investigation due to the substantial consequences of aerosol explosions. Furthermore, it acknowledges the limited understanding of flammable mist formation and the corresponding determination of hazardous areas—these gaps in knowledge warrant further scrutiny.[8]

n-Decane ($C_{10}H_{22}$) is a highly versatile energetic material derived from hydrocarbon fuels, with diverse applications. Its utility spans from serving as a potent liquid explosive to functioning as a solvent for chemical processing and analysis.[9] Furthermore, it has demonstrated remarkable potential as a high-performance fuel additive for internal combustion engines.[10] However, the widespread adoption of *n*-decane as an energy carrier is impeded by critical safety concerns that necessitate resolution before achieving social acceptance.[11−13] This fuel's production, handling, transportation, and storage tail inherent explosion hazards that demand meticulous attention and adequate mitigation measures.[14−17] Instances such as fuel spray resulting from broken pipelines or containers have the potential to induce severe accidents,[18] including fires, explosions, and the deflagration to detonation transition (DDT) phenomenon.[19−21]

At atmospheric pressure and standard temperature, the flammability limits of gaseous *n*-decane in air range from 0.78 to 7.8%. Furthermore, the saturated vapor pressure of *n*-decane is approximately 0.13 kPa, corresponding to a vapor-phase concentration of about 0.13%.[22,23] Upon ignition, given that the ambient temperature typically reaches room temperature, a combination of vapor-phase premixed explosion and liquid-phase diffusive combustion of *n*-decane aerosols coexist. It is noteworthy, however, that limited attention has been devoted to studying variations in the flammability limit of *n*-decane aerosols in air. Additionally, previous literature lacks exploration into the influence of the liquid-phase particle size on explosion parameters concerning *n*-decane.

Hence, this study addresses the gaps in the research mentioned above by investigating the flammability limit of *n*-decane aerosols in air and comprehensively examining the effect of liquid-phase particle size on explosion parameters. By delving into these aspects, we can attain a more thorough understanding of the safety considerations associated with the use of *n*-decane

Received: July 13, 2023
Revised: January 10, 2024
Accepted: January 11, 2024
Published: January 31, 2024

as an energy carrier. The findings from this research will contribute to developing robust safety protocols and guidelines, paving the way for the broader utilization of *n*-decane as an energy resource while ensuring a secure and sustainable energy landscape.

Table 1 presents a comprehensive overview of the physicochemical properties and flammability characteristics of *n*-decane. This study aims to investigate the impact of two distinct sets of aerosol/air mixtures containing *n*-decane, characterized by mean Sauter mean diameters (SMDs) of 22 and 38 μm on key explosion parameters. Specifically, the study aims to measure and analyze the lower flammability limit (LFL), peak pressure, and peak temperature associated with these mixtures.

Table 1. Physicochemical Properties and Flammability Characteristics of *n*-Decane

liquid hydrocarbon fuel	*n*-decane
chemical formula	$C_{10}H_{22}$
density (water = 1 g/cm^3) at 293 K	0.730
boiling point (K)	447.3
flash point (K)	319
saturated vapor pressure at 20 °C (%) (kMP)	0.13
explosion limits at 20 °C (%) (v/v)	0.78−7.8
dynamic viscosity at 20 °C (Pa·s)	0.00093
surface tension at 20 °C (mN/m)	25.80
autoignition temperature (°C)	483
heat of combustion (kJ/mol)	6730.6

Rigorous experimental procedures were implemented to ensure accurate and reliable data collection.[24−27] The LFL, which indicates the minimum concentration of *n*-decane aerosol in the air required to sustain combustion, was determined for each mixture. The peak pressure and peak temperature resulting from the combustion process were also quantified and compared across different concentrations. The qualitative and quantitative results underwent meticulous analysis, considering the influence of SMDs and concentration on the explosion parameters.

The findings from this study contribute to a deeper understanding of the behavior of *n*-decane aerosol/air mixtures in terms of their flammability characteristics. The results shed light on the LFL, peak pressure, and peak temperature as critical indicators of the potential hazards associated with varying concentrations of *n*-decane. These insights have implications for risk assessment and safety measures in industrial settings, where *n*-decane is handled or stored.

2. EXPERIMENTAL APPARATUS AND PROCEDURES

2.1. Equipment. The experimental investigations used two specially designed spherical vessels, each with a volume of 20 L. These vessels were carefully selected to serve distinct purposes in the study. The first vessel, depicted in Figure 1a, was constructed using 5 mm-thick plexiglas, chosen for its optical properties that facilitated the implementation of an advanced concentration and particle size detection system, as well as a particle image velocimetry (PIV) detection system. Using plexiglas ensured the accurate capture of optical signals, contributing to precise measurements and analysis. The PIV experiments closely followed the steps outlined in El-Zahlanieh et al.,[28] concerning the utilization of a continuous-wave laser operating at a wavelength of 532 nm, powered by a neodymium-doped yttrium aluminum garnet (Nd:YAG) system. This laser was instrumental in illuminating dispersed liquid droplets, enabling precise tracking of their movement, a process captured meticulously at a rate of 2000 frames/s using the high-speed camera, specifically the Phantom VEO 410L model. Subsequent data extraction, analysis, and validation were carried out consistently with the methodologies described in PIVlab version 2.45, as elucidated by El-Zahlanieh et al.[28]

The second vessel, depicted in Figure 1b, employed a different construction material. A 10 mm-thick stainless steel vessel was utilized to conduct experiments about explosion parameters. Stainless steel was chosen for its high strength and durability, ensuring the containment of the explosive forces generated during the experiments. This vessel was specifically designed to withstand the intense pressures and temperatures associated with the ignition and subsequent explosion phenomena under investigation.

Temperature measurements were conducted using Kaipusen's B-type platinum−rhodium (Pt−Rh) sheathed thermocouples with sapphire protection, specifically designed to operate within a temperature range of 0−1800 °C. Pressure measurements were carried out with Shuangqiao's CYG1401F-JBS13C2A1 pressure sensor, offering a measurement range of 0−1 MPa and demonstrating remarkable accuracy, with a margin of 0.25%. The utilization of these precise temperature and pressure sensors facilitated the precise quantification of the peak pressure and peak temperature during the entire combustion process.

To ensure synchronized and controlled execution of the experiments, we implemented a trigger control system. This system acted as a regulator for double-nozzle pneumatic atomization and electric ignition systems. The experimental conditions could be accurately reproduced by precise timing and coordination of these two components, enabling consistent data acquisition and analysis.

The ignition process was achieved within the spherical explosion vessel using a spark discharge ignition mechanism. This involved the placement of tungsten electrodes with rounded tips close to each other. The separation distance between the electrode tips, called the spark gap, was maintained at a fixed value of 1 mm. The spark discharge between these electrodes initiated the ignition, enabling a controlled release of energy within the vessel. In this work, we implemented a siphon-gravity feed spray system, inspired by the work of El-Zahlanieh et al.[28] This system consisted of a Venturi tee featuring dual inlets: one connected to a compressed air cylinder to serve as the air inlet and the other linked to a fuel container maintained at room temperature to act as the liquid inlet. The fine-tuning of the aerosol cloud's flow rate and the distribution of droplet sizes were achieved by adjusting the two nozzles/caps within the spray system, thereby enabling modifications to the initial conditions, as suggested by El-Zahlanieh et al.[28] and Wang.[29]

For further information on the specific details of the experimental setup, readers are referred to our previous study.[30] This prior work provides a comprehensive description of the experimental apparatus, including the configuration of the vessels, the intricate components of the trigger control system, and the precise procedures employed to ensure reliable and consistent testing conditions.

2.2. Liquid Phase *n*-Decane Concentration Measurements. This study focuses on characterizing the behavior of a solenoid valve during a consistent 50 ms opening period, which corresponds to the spray time. A key parameter of interest is the ignition delay time (IDT), which represents the duration

https://doi.org/10.1021/acsomega.3c05036
ACS Omega 2024, 9, 6381−6390

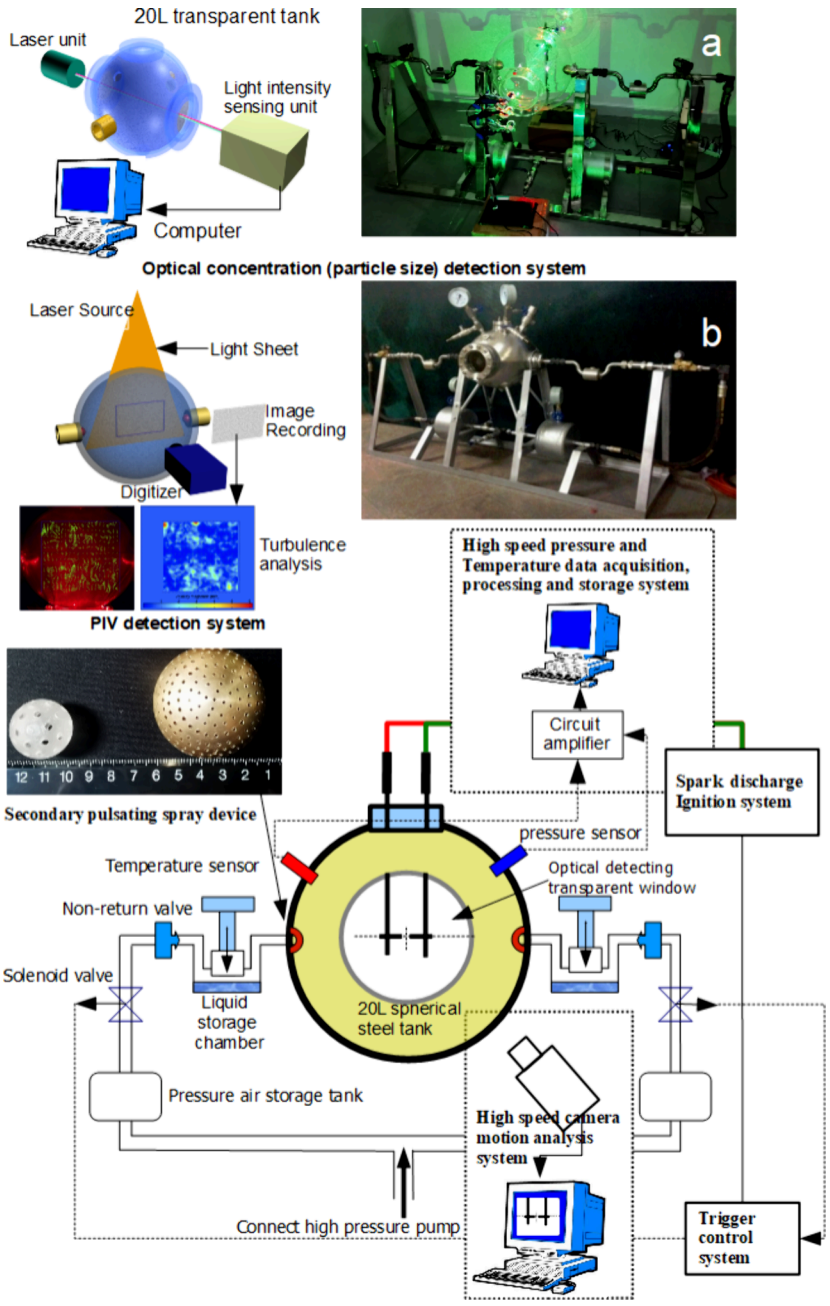

Figure 1. Experimental setup: (a) plexiglass container and (b) stainless steel container.

between the initiation time of the spray (ITS) and the initiation time of ignition (ITI). To accurately determine the IDT, it is crucial to employ homogeneous *n*-decane/air mixtures, which is an established approach in the field. To capture and analyze the spray process, a combination of image collection techniques and Mie extinction detection methods was employed. The experimental setup consisted of high-speed imaging equipment capable of capturing rapid events with precision. The image collection process enabled visual examination and documentation of the spray behavior. Additionally, Mie extinction detection techniques were utilized to measure the particle concentration in the spray, facilitating quantitative analysis of the experimental data. The IDT was predetermined to be 100 ms to ensure consistency and reliability as established in previous studies (refer to ref 31 for comprehensive details on the methodology used for this determination).

In preparation for the experiments, two parameters, namely, the design spray dose (DSD) and loss spray dose (LSD), were introduced to quantify the concentration of liquid *n*-decane in two liquid storage chambers and the concentration of residual liquid in those chambers, respectively. By manipulation of the pneumatic atomization pressure via a high-pressure pump and adjustment of the DSD of liquid *n*-decane, a sampling time of 100 ms was achieved. The Mie extinction detection system was utilized throughout the study to accurately measure the real-time concentrations and SMDs of liquid-phase *n*-decane at the moment of ignition. The concentrations of vapor-phase *n*-decane were derived from the saturated vapor pressure of *n*-decane, resulting in a vapor-phase concentration of 0.13%. Furthermore, to assess wall loss, a nonevaporable liquid (glycerin) spray test was conducted. By employing real-time detection using the Mie extinction detection system at the

https://doi.org/10.1021/acsomega.3c05036
ACS Omega 2024, 9, 6381−6390

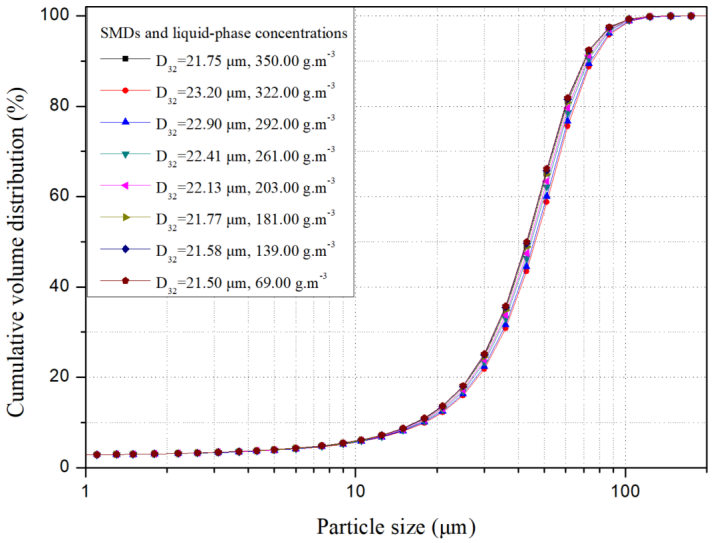

(a) Particle size distributions of various concentrations at a mean SMD of 22 μm.

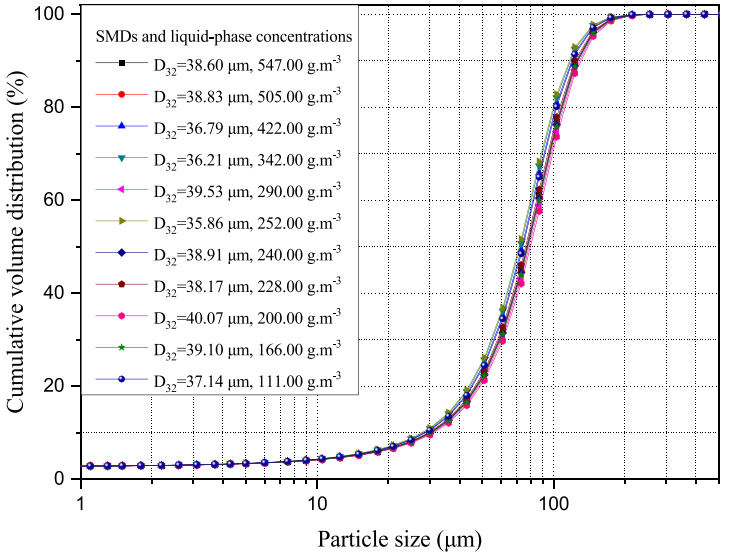

(b) Particle size distributions of various concentrations at a mean SMD of 38 μm.

Figure 2. Particle size distribution of *n*-decane at different concentrations and 100 ms sampling time nodes.

Table 2. Experiment Data of SMD and Concentration of the *n*-Decane at a Mean SMD of 22 *μ*m

					mean value	
pneumatic pressure, MPa	pressure of 80 ms time node, MPa	DSD, g/m^3	LSD, g/m^3	liquid phase concentration, g/m^3	mean SMD, μm	saturated vapor, %
0.80	0.104	438.00	88.00	350.00	21.75	0.13
0.80	0.104	402.00	80.00	322.00	23.20	
0.80	0.103	365.00	73.00	292.00	22.90	
0.70	0.103	292.00	29.00	261.00	21.63	
0.65	0.102	226.00	23.00	203.00	21.00	
0.65	0.102	190.00	9.00	181.00	20.99	
0.60	0.102	146.00	7.00	139.00	21.58	
0.60	0.103	73.00	4.00	69.00	21.50	

ignition time point (100 ms), it was determined that the disparity between the real-time detection and spray concentrations ranged from 8 to 12%. Consequently, the wall loss was estimated to be 10%.

The significance of the SMD was emphasized in this study.[32] Given the relatively minor fluctuations observed in the SMD, it was deemed feasible to treat it as a constant. This simplification greatly facilitated the assessment of concentration's impact on the explosion parameters of *n*-decane/air mixtures.[33] The

https://doi.org/10.1021/acsomega.3c05036
ACS Omega 2024, 9, 6381−6390

Table 3. Experiment Data of SMD and Concentration of the *n*-Decane at a Mean SMD of 38 μm

					mean value	
pneumatic pressure, MPa	pressure of 80 ms time node, MPa	DSD, g/m^3	LSD, g/m^3	liquid phase concentration, g/m^3	mean SMD, μm	saturated vapor, %
0.80	0.104	730.00	183.00	547.00	38.60	0.13
0.75	0.104	672.00	167.00	505.00	38.83	
0.70	0.103	555.00	133.00	422.00	36.79	
0.60	0.103	475.00	133.00	342.00	36.21	
0.50	0.103	402.00	112.00	290.00	39.53	
0.50	0.103	365.00	113.00	252.00	35.86	
0.50	0.103	329.00	89.00	240.00	38.91	
0.50	0.103	292.00	64.00	228.00	38.17	
0.50	0.103	256.00	56.00	200.00	40.07	
0.45	0.102	219.00	53.00	166.00	39.10	
0.45	0.102	146.00	35.00	111.00	37.14	

Table 4. Experimental Results for *n*-Decane Aerosols at a Mean SMD of 22 μm[a]

liquid phase concentration, g/m^3	saturated vapor, %	experiment times, F/S	maximum pressure, MPa	maximum temperature, °C
350.00	0.13	3(S)	0.86	902
322.00		3(S)	0.79	920
292.00		3(S)	0.74	962
261.00		3(S)	0.68	920
203.00		3(S)	0.56	780
181.00		1(S) 2(F)	0.51	644
139.00		3(F)	/	/
69.00		3(F)	/	/

[a]"F" and "S" denote "failure" and "success", respectively. 3(S) denotes that the tests were repeated three times. The maximum pressure and temperature are the mean values of the 3(S) tests.

Table 5. Experimental Results for *n*-Decane Aerosols at a Mean SMD of 38 μm[a]

liquid phase concentration, g/m^3	saturated vapor, %	experiment times, F/S	maximum pressure, MPa	maximum temperature, °C
547.00	0.13	3(S)	0.90	723
505.00		3(S)	0.97	726
422.00		3(S)	0.85	750
342.00		3(S)	0.74	812
290.00		3(S)	0.65	760
252.00		3(S)	0.60	720
240.00		3(S)	0.58	701
228.00		3(S)	0.56	674
200.00		1(S) 2(F)	0.52	630
166.00		3(F)	/	/
111.00		3(F)	/	/

[a]"F" and "S" denote "failure" and "success", respectively. 3(S) denotes that the tests were repeated three times. The maximum pressure and temperature are the mean values of the 3(S) tests.

particle size distribution, as depicted in Figure 2, was determined at the ignition location and consistently exhibited values averaging at 22 and 38 μm. To accumulate a substantial volume of empirical data, a comprehensive series of experiments was conducted, and specific details are provided in Tables 2 and 3.

2.3. Experimental Ignition Procedure. In this set of experiments, meticulous control was exercised over the environmental conditions to ensure accuracy and consistency of the results. The initial temperature and pressure of the *n*-decane/air mixtures were precisely set to 21 °C and 0.1 MPa, respectively. Two air chambers were utilized to facilitate the storage of high-pressure gas. The liquid *n*-decane was accurately deposited within the storage chambers. To commence the experiment, the central control system was initialized in the first instance. The solenoid valve was programmed to open for a duration of 50 ms, while the IDT was established at 100 ms. Once all of the essential parameters had been configured, the central control system was activated, inducing the ignition of the *n*-decane/air mixtures through an electric spark generated by a dedicated spark generator. Subsequently, following the ignition of the *n*-decane aerosols, a combustion wave was meticulously observed, propagating from the ignition point toward the vessel wall. This phenomenon was closely monitored and subjected to analysis throughout the entire duration of the experiment. Pressure gauges and temperature transducers, connected to a data acquisition system, were strategically positioned at various locations within the vessel to capture and record the temporal evolution of the pressure and temperature resulting from the explosion of the *n*-decane/air mixtures. By employing this experimental setup, we were able to amass valuable data pertaining to the explosion characteristics of *n*-decane/air mixtures. The recorded pressure and temperature histories

https://doi.org/10.1021/acsomega.3c05036
ACS Omega 2024, 9, 6381−6390

offer profound insights into the dynamics and behavior of the combustion process, thereby contributing to a more comprehensive understanding of the subject matter.

3. EXPERIMENTAL RESULTS AND DISCUSSION

3.1. Flame Temperatures and Explosion Pressures.

Initiation energy plays a vital role in the process of flame propagation and serves to prevent the immediate extinction of vapor−liquid two-phase fuel/air mixtures.[34] Therefore, in our experimental setup, spark ignition was employed to ensure reliable and sustained ignition and flame propagation. The ignition energy was kept constant at 40.32 J ($CU^2/2$). The experiments were conducted with varying mass concentrations of *n*-decane in the liquid phase, ranging from 69 to 350 g/m^3, while a fixed concentration of 0.13% was maintained in the saturated vapor phase. These conditions corresponded to a total mean SMD of 22 μm. Furthermore, experiments were performed with mass concentrations of *n*-decane in the liquid phase ranging from 111 to 547 g/m^3, along with the same concentration of 0.13% in the saturated vapor phase, resulting in a total mean SMD of 38 μm.

As the SMD and *n*-decane concentrations were measured, temporal variations in pressure and temperature were observed, with peaks occurring after the passage of pressure and temperature waves. The peak pressure and peak temperature are the highest values that the pressure and temperature have ever reached. Importantly, these peak values exhibited variations corresponding to the concentration of *n*-decane. A comprehensive summary of the experimental results is presented in Tables 4 and 5.

Figure 3 shows the relationship between peak pressure and vapor-phase concentrations of *n*-decane aerosols across different

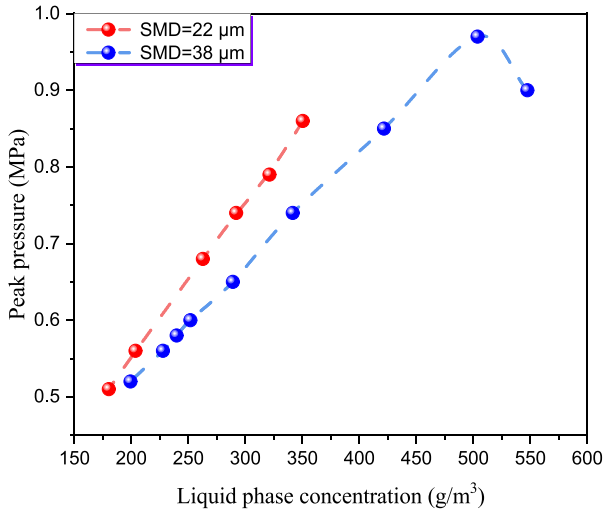

Figure 3. Trend of the peak pressure at various concentrations of the *n*-decane aerosol.

scenarios. When considering a mean SMD of 22 μm, the peak pressure exhibits a gradual increase from 0.53 to 0.86 MPa within the liquid-phase concentration range of 69−350 g/m^3. Similarly, for a mean SMD of 38 μm, the peak pressure rises from 0.52 to 0.97 MPa as the liquid-phase concentration ranges from 111 to 505 g/m^3. Notably, within the concentration range of 505−547 g/m^3, the peak pressure experiences a subsequent decline from 0.97 to 0.90 MPa.

Moving on to Figure 4, we observe the peak temperatures associated with various concentrations of *n*-decane aerosols at

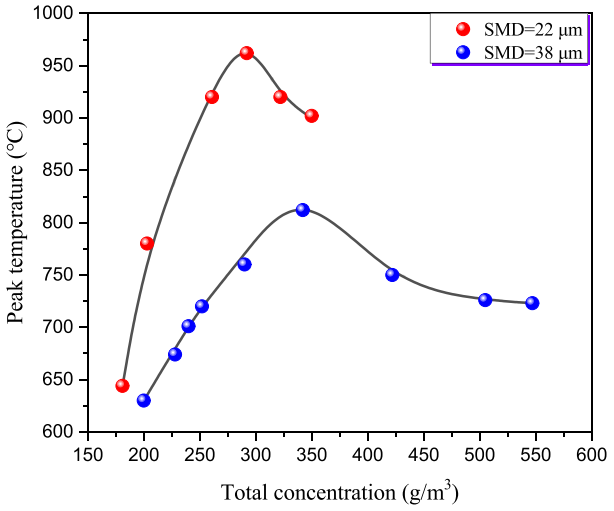

Figure 4. Trend of the peak temperature at various concentrations of the *n*-decane aerosol.

mean SMD values of 22 and 38 μm. For the former, the maximum and minimum peak temperatures are recorded as 962 and 644 °C, respectively. As for the latter, the peak temperatures reach a maximum of 812 °C while the minimum value remains constant at 630 °C.

Based on the findings presented in Figure 4, it is evident that the peak temperature is higher for a mean SMD of 22 μm compared to 38 μm. Previous literatures[35−42] also support the synchronization of peak pressures and peak temperatures in pure gaseous fuel/air mixtures. However, tests conducted at a mean SMD of 38 μm reveal that the concentration yielding the maximum peak pressure for *n*-decane exceeds the maximum peak temperature. Based on these observations, the following conclusions can be drawn:

(1) Regarding the maximum peak temperature, an increase in lean concentration adversely affects the transient burn process and the diffusion-combustion process. This adverse effect can primarily be attributed to the droplet size distribution and the specific surface area of the droplets in the air, which play a crucial role in heat absorption and the cooling effect on unburned and partially burned droplets during the reaction process. At the concentration associated with the maximum peak temperature, the explosion reaction can be considered to have reached its optimal state. At this point, the proportion of endothermic droplets is at its lowest, resulting in a combustion ratio that is most favorable for *n*-decane aerosol/air mixtures. However, this concentration does not lead to complete oxygen depletion, indicating that the oxygen is not fully consumed.[43]

(2) Concerning the maximum peak pressure, an increase in concentration leads to a gradual increase in the specific surface area of the droplet group in the air. Consequently, a larger number of droplets are involved in the transient combustion reaction. This eventually results in complete oxygen depletion and the occurrence of the maximum peak overpressure. The concentration associated with this peak pressure signifies the highest output energy,

https://doi.org/10.1021/acsomega.3c05036
ACS Omega 2024, 9, 6381−6390

representing the optimal oxygen consumption concentration.

By examination of the relationship between concentration and the maximum peak temperature and pressure, it becomes apparent that different concentration levels yield distinct combustion characteristics for *n*-decane aerosol/air mixtures. Understanding these phenomena is crucial for achieving efficient and environmentally friendly combustion processes.

3.2. LFL. Previous studies in the literature have primarily focused on investigating the impact of particle size on the flammability limit in both nearly quiescent and momentum-dominated spray environments.[44−50] However, in momentum-dominated sprays, the behavior of the LFL with respect to the droplet size differs from that of quiescent mists. Several experiments conducted by Rao and Lefebvre[47] as well as Anson[46] have shown that, in momentum-dominated sprays, the LFL tends to increase as the droplet size increases. It should be noted that this behavior is observed when the flow speed exceeds 15 m/s, where the influence of sedimentation becomes relatively insignificant compared to the droplet velocity. Nevertheless, it is essential to analyze the concentration of the saturated vapor pressure at the moment of ignition. In our present investigation, we examine the turbulence velocity (Urms), which exhibits fluctuations ranging from 3.5 to 7 m/s at an ignition time of 100 ms.[30] This parameter plays a crucial role in this analysis and provides valuable insights into the dynamics of the system under study.

This study delves into the concept of "experimental iterations" as a metric for the number of times an experiment was repeated. The terms "F″ and "S″ denote "failure" and "success", respectively, indicating whether the mixture in the vessel failed to initiate or successfully exploded during the experiment. More specifically, the determination of the LFL of *n*-decane aerosols relies on a combination of "successful ignition-1(S)2(F)″ and "failed ignition-3(F)″ events. Experimental analysis was conducted to ascertain the LFLs of *n*-decane aerosols under saturated vapor pressure, yielding values of 181 g/m^3 at a mean SMD of 22 μm and 200 g/m^3 at a mean SMD of 38 μm, as illustrated in Figure 5.

This study centers around the phenomenon observed when larger droplets fail to fully vaporize before being consumed by the advancing flame front. Consequently, each droplet undergoes combustion with its diffusion flame rather than participating in a homogeneous gaseous-phase mixture.[51] The primary mechanism of flame propagation in this context involves the transfer of heat from one burning droplet to the neighboring droplets. Two key aspects are particularly emphasized: First, droplets with an SMD exceeding 20 μm do not have adequate time for complete vaporization. Second, heat transfer within the droplets absorbs thermal energy and decelerates the speed of flame propagation, thereby rendering ignition more challenging and consequently increasing the LFL.

3.3. Flame Propagation Delay Time. Examining aerosols during the explosion process under saturated vapor pressure presents a complex and interdisciplinary challenge. This phenomenon encompasses various aspects, such as heat and mass transfer, fluid dynamics, and chemical kinetics. A crucial element of this process entails determining both the flame propagation delay time and the overpressure rise time, as shown in Figure 6. Throughout this investigation, a fixed IDT of 100 ms is employed. The flame propagation delay time emerges as a prominent characteristic, particularly in turbulent environments.[52] Referring to Figure 7, it is evident that when an ignition and flame propagation process occurs with an aerosol

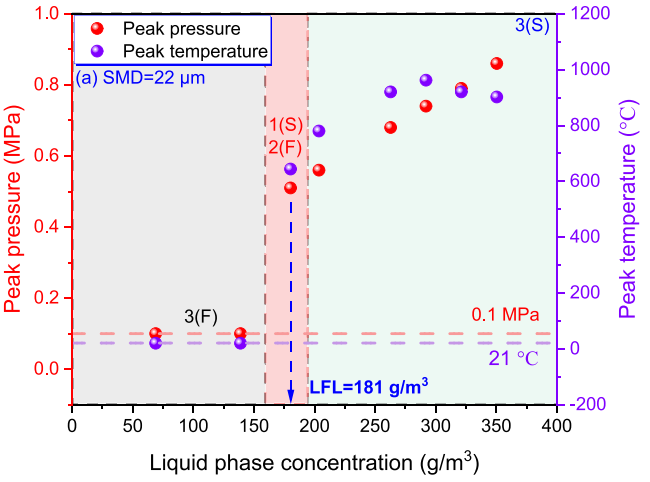

(a) Lower flammability limit of n-decane aerosol at SMD=22 μm

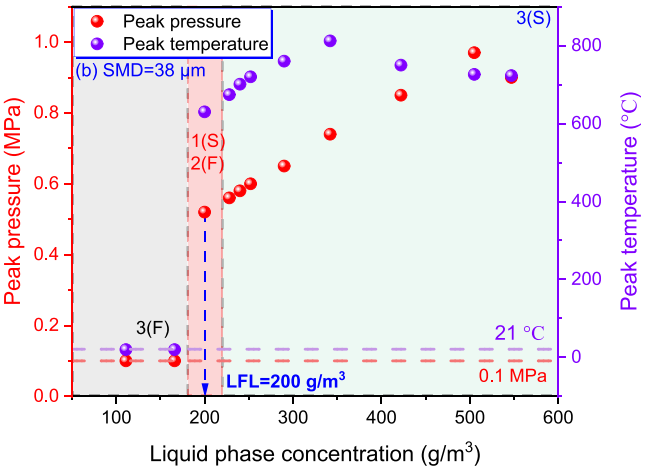

(b) Lower flammability limit of n-decane aerosol at SMD=38 μm

Figure 5. Lower flammability limit of *n*-decane: (a) lower flammability limit of *n*-decane aerosol at SMD = 22 μm, (b) lower flammability limit of *n*-decane aerosol at SMD = 38 μm.

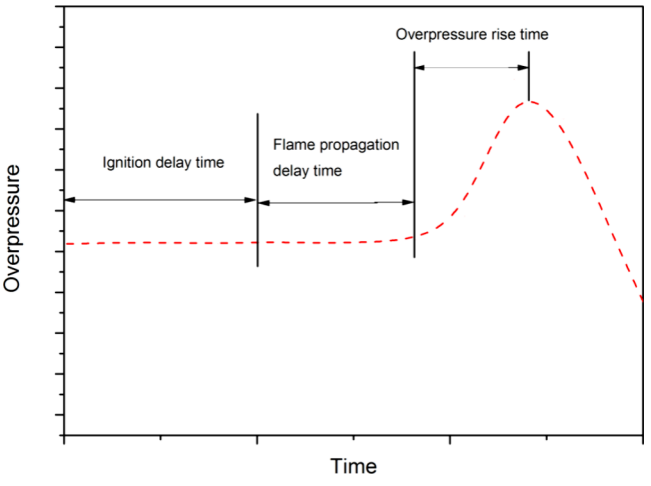

Figure 6. Vapor−liquid two-phase explosion process.

https://doi.org/10.1021/acsomega.3c05036
ACS Omega 2024, 9, 6381−6390

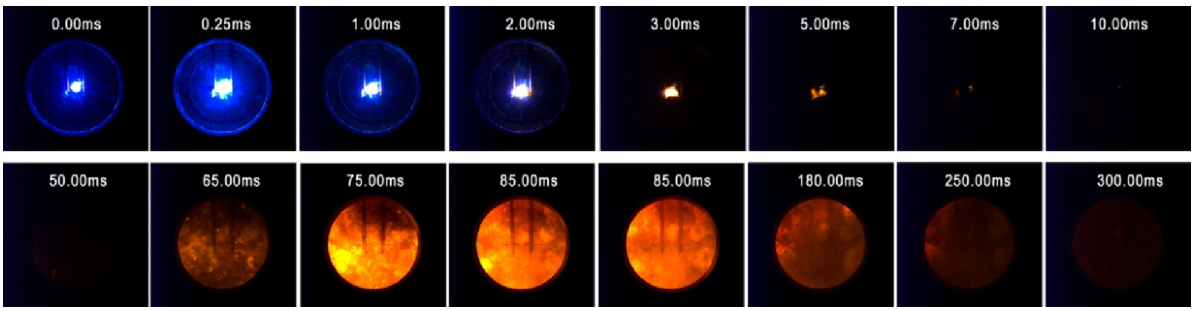

Figure 7. Ignition and flame propagation process of 262.8 g/m^3 at an SMD of 22 μm.

concentration of 292 g/m^3 and a surface mean diameter (SMD) of 22 μm, the flame propagation delay time is recorded as 50 ms.

Figure 8 illustrates the relationship between the flame propagation delay time and concentration for two distinct

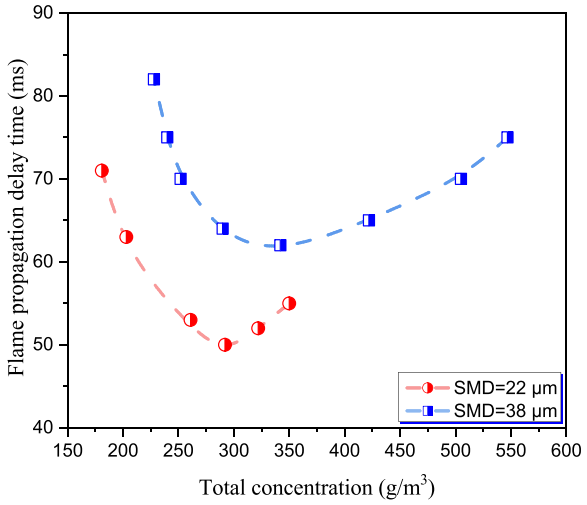

Figure 8. Flame propagation delay time vs concentration for the two groups with different SMDs.

groups characterized by varying SMDs. Upon analyzing the presented data, the following conclusions can be drawn:

(1) With an increase in the concentration of the liquid phase, the flame propagation delay time initially decreases before subsequently increasing.

(2) Furthermore, an increase in SMD results in a proportional increase in the flame propagation delay time. Moreover, an examination of Figures 4 and 8 uncovers a correlation between the peak temperature and flame propagation delay time. Specifically, when the flame propagation delay time reaches its minimum value, the corresponding peak temperature reaches its maximum value.

4. CONCLUSIONS

This work investigated *n*-decane aerosols at various concentrations under saturated vapor pressures with mean SMDs of 22 and 38 μm. The analysis of explosion parameters for different SMDs leads to several qualitative conclusions. First, smaller SMDs result in higher peak pressures and temperatures than larger SMDs at the same concentration. Second, the concentration required to produce the maximum peak pressure of *n*-decane is higher than that needed to achieve the maximum peak temperature, regardless of particle size. Third, as the SMD increases, the flame propagation delay time also increases, and at the point where the delay time is minimized, the corresponding peak temperature is maximized.

Furthermore, several quantitative conclusions have also been derived from the work. First, the LFL of *n*-decane aerosols under saturated vapor pressure occurs at a liquid-phase concentration of 181 g/m^3 for a mean SMD of 22 μm and at 200 g/m^3 for a mean SMD of 38 μm. Second, at an ignition energy of 40.32 J, the maximum peak pressure observed was 0.97 MPa, corresponding to a total concentration of 505 g/m^3 for a mean SMD of 38 μm in all experiments. Third, under the same total concentration conditions, the peak temperature at a mean SMD of 22 μm exceeds that at a mean SMD of 38 μm. Notably, the maximum temperature recorded was 962 °C at a total concentration of 292 g/m^3 for a mean SMD of 22 μm. In comparison, it reached 812 °C at a total concentration of 342 g/m^3 for a mean SMD of 38 μm in all of the experiments conducted.

Overall, this study provides valuable insights into the explosion characteristics of *n*-decane aerosols, shedding light on the influence of particle size and concentration on the peak pressure, peak temperature, and flame propagation delay time. These findings contribute to our understanding of aerosol behavior in explosive environments and have practical implications for safety measures in various industries.

AUTHOR INFORMATION

Corresponding Author

Chang Qi − *School of Chemical Engineering, Dalian University of Technology, Dalian 116024, China;* orcid.org/0000-0003-4862-7817; Phone: +86 13023518011; Email: qichang621@hotmail.com

Authors

Yue Wang − *Key Laboratory of Coal Resources and Green Mining in Xinjiang, Ministry of Education, Xinjiang Institute of Engineering, Urumqi 830023, China*

Xueling Liu − *School of Physics and Engineering Technology, Xingyi Normal University for Nationalities, Xingyi 562400, China;* orcid.org/0000-0001-6478-202X

Complete contact information is available at: https://pubs.acs.org/10.1021/acsomega.3c05036

Author Contributions

The manuscript was written through contributions of all authors. All authors have given approval to the final version of the manuscript.

Funding

This work was supported by the National Natural Science Foundation of China (No.21865036), State Key Laboratory of

Coal Resources and Safe Mining-Xinjiang Institute Engineering Joint Open Research Fund Project (No.SKLCRSM-XJIEKF007).

Notes

The authors declare no competing financial interest.

■ ACKNOWLEDGMENTS

This work was supported by the National Natural Science Foundation of China (No. 21865036) and the State Key Laboratory of Coal Resources and Safe Mining-Xinjiang Institute Engineering Joint Open Research Fund Project (No. SKLCRSM-XJIEKF007).

■ REFERENCES

(1) Lees, P.; Gant, S.; Bettis, R.; Vignes, A.; Lacome, J.-M.; Dufaud, O., Eds. *Review of recent incidents involving flammable mists*, IChemE Hazards 2019.

(2) Yuan, S.; Ji, C.; Han, H.; Sun, Y.; Mashuga, C. V. A review of aerosol flammability and explosion related incidents, standards, studies, and risk analysis. *Process Saf. Environ. Prot.* **2021**, *146*, 499−514.

(3) Yuan, S.; Zhang, Z.; Sun, Y.; Kwon, J. S.-I.; Mashuga, C. V. Liquid flammability ratings predicted by machine learning considering aerosolization. *J. Hazard. Mater.* **2020**, *386*, 121640.

(4) Gant, S.; Bettis, R.; Santon, R.; Buckland, I.; Bowen, Phil; Kay, P.Generation of flammable mists from high flashpoint fluids: literature review. *Health and Safety Executive, Research Report RR980*; **2013**.

(5) *Explosive atmospheres. Part 10−1, Classification of areas. Explosive gas atmospheres*; British Standards Institution: London.

(6) Toman, A.; Adamus, W. Explosive properties of selected aerosols determined in a spherical 5-L test chamber. *J. Loss Prev. Process Ind.* **2023**, *82*, 104992.

(7) *Area classification code for installations handling flammable fluids:Part 15 of the IP model code of safe practice in the petroleum industry*, 4th ed.; Energy Institute, 2015.

(8) Santon, R., Ed. *Mist fires and explosions-an incident survey*; IChemE Hazards XXI Symposium & Workshop 2009.

(9) Hartmann, M.; Elangovan, S. Isomerization and Hydrocracking of n-Decane over Magnesium-Containing Molecular Sieves with AEL, AFI, and AFO Topology. *Chem. Eng. Technol.* **2003**, *26* (12), 1232−1235.

(10) Soid, S. N.; Zainal, Z. A. Spray and combustion characterization for internal combustion engines using optical measuring techniques − A review. *Energy* **2011**, *36* (2), 724−741.

(11) Xu, C.; Wang, Q.; Song, Y.; Liu, K.; Li, X. Explosion characteristics of n-decane/hydrogen/air mixtures. *Int. J. Hydrogen Energy* **2022**, *47* (91), 38837−38848.

(12) Shao, X.; Zhao, N.; Zheng, H. Effects of inlet total pressure on the formation and propagation characteristics of n-decane two-phase rotating detonation waves. *Aerosp. Sci. Technol.* **2023**, *138*, 108317.

(13) Song, Y.; Zhang, Q. Explosion effect of vapor-liquid two-phase n-heptane at various initial temperatures. *Process Saf. Environ. Prot.* **2021**, *145*, 303−311.

(14) El-Zahlanieh, S.; Charvet, A.; Vignes, A.; Tribouilloy, B.; Dufaud, O. Hydrocarbon aerosol explosion: towards hazardous area classification. In *13th International symposium on hazards, prevention, and mitigation of industrial explosions*; 2020; pp 572−583 DOI: 10.7795/810.20200724.

(15) El-Zahlanieh, S.; Jean, A.; Vignes, A.; Dufaud, O., Eds. The role of vapor fraction in hydrocarbon mist explosion, *14th International Symposium on Hazards, Prevention, and Mitigation of Industrial Explosions (ISHPMIE 2022)*; Physikalisch-Technische Bundesanstalt (PTB) 2022.

(16) El-Zahlanieh, S.; Sivabalan, S.; Dos Santos, I. S.; Tribouilloy, B.; Brunello, D.; Vignes, A.; Dufaud, O. A step toward lifting the fog off mist explosions: Comparative study of three fuels. *J. Loss Prev. Process Ind.* **2022**, *74*, 104656.

(17) Cammarota, F.; Di Benedetto, A.; Di Sarli, V.; Salzano, E. Influence of initial temperature and pressure on the explosion behavior of n-dodecane/air mixtures. *J. Loss Prev. Process Ind.* **2019**, *62*, 103920.

(18) Yao, G.; Zhang, B.; Xiu, G.; Bai, C.; Liu, P. The critical energy of direct initiation and detonation cell size in liquid hydrocarbon fuel/air mixtures. *Fuel* **2013**, *113*, 331−339.

(19) Sun, K.; Zhang, Q.; Wang, W.; Niu, S. Experimental study on explosion parameters of ethanol aerosol under high-temperature source ignition. *Fuel* **2022**, *311*, 122610.

(20) Sun, K.; Zhang, Q. Effect of nitroethane on explosion parameters of multi-component mixed fuel aerosol. *Fuel* **2022**, *320*, 123897.

(21) Yuan, S.; Ji, C.; Monhollen, A.; Kwon, J. S.-I.; Mashuga, C. Experimental and thermodynamic study of aerosol explosions in a 36 L apparatus. *Fuel* **2019**, *245*, 467−477.

(22) Affens, W. A. Flammability Properties of Hydrocarbon Fuels. Interrelations of Flammability Properties of n-Alkanes in Air. *J. Chem. Eng. Data* **1966**, *11* (2), 197−202.

(23) Zabetakis, M. G.; Scott, G. S.; Jones, G. W. Limits of Flammability of Paraffin Hydrocarbons in Air. *Ind. Eng. Chem.* **1951**, *43* (9), 2120−2124.

(24) Qi, C.; Yu, X.; Wang, Y.; Chen, L.; Yan, X.; Lv, X.; Liang, H.; Yu, J. Investigating the effect of temperature, pressure, and inert gas on the flammability range of ethane/oxygen mixtures. *Fuel* **2023**, *354*, 129296.

(25) Qi, C.; Yan, X.; Wang, Y.; Ning, Y.; Yu, X.; Hou, Y.; Lv, X.; Ding, J.; Shi, E.; Yu, J. Flammability limits of combustible gases at elevated temperatures and pressures: recent advances and future perspectives. *Energy Fuels* **2022**, *21* (36), 12896−12916.

(26) Qi, C.; Ding, J.; Wang, Y.; Ning, Y.; Wang, Y.; Liang, H.; Yan, X.; Yu, J. Investigation of the upper flammability limit of ethylene/propane mixtures in air at high temperatures and pressures. *Energy* **2023**, *285*, 128114.

(27) Qi, C.; Wang, Y.; Ning, Y.; Shi, E.; Yan, X.; Lv, X.; Yu, J. Investigation on the upper flammability limits of ethylene/air and propane/air mixtures at high temperature and pressure. *J. Energy Inst.* **2023**, *109*, 101291.

(28) El-Zahlanieh, S.; Dos Santos, I. S.; Sivabalan, S.; Brunello, D.; Tribouilloy, B.; Vignes, A.; Dufaud, O. Finding a way through the "misty" evaluation of the flammability and explosivity of kerosene aerosols. *Fuel* **2022**, *328*, 125275.

(29) Wang, Y. *Research on generation of mists and explosion characteristics for flammable liquid fuels*; Beijing Institute of Technology; Doctor: Beijing, 2016.

(30) Wang, Y.; Li, W.; Chang, Q.; Cheng, J. Measurements of explosion parameters for diethyl ether/air mixtures at pre-ignition quasi-isotropic turbulence. *Fuel* **2021**, *292*, 120224.

(31) Liu, X.; Wang, Y.; Zhang, Q. A study of the explosion parameters of vapor-liquid two-phase JP-10/air mixtures. *Fuel* **2016**, *165*, 279−288.

(32) Sun, K.; Zhang, Q. Experimental study on the vapor-liquid two-phase explosion of n-heptane under high-temperature source ignition. *Combust. Flame* **2021**, *234*, 111633.

(33) Meng, Q.; Zhao, N.; Zhang, H. On the distributions of fuel droplets and in situ vapor in rotating detonation combustion with prevaporized n-heptane sprays. *Phys. Fluids (1994)* **2021**, *33* (4), 43307.

(34) Schmiermund, T. *The Chemistry Knowledge for Firefighters*; Springer: Berlin, Heidelberg, 2023. DOI: 10.1007/978-3-662-64423-2_39.

(35) Liu, X.; Zhang, Q.; Wang, Y. Influence of Vapor−Liquid Two-Phase n -Hexane/Air Mixtures on Flammability Limit and Minimum Ignition Energy. *Ind. Eng. Chem. Res.* **2014**, *53* (32), 12856−12865.

(36) Liu, X.; Wang, Y. A Comparative Study of the Explosion Characteristics of IPN and IPN/JP-10 Mixtures in Air Aerosols. *Propellants, Explosives, Pyrotechnics* **2017**, *42* (10), 1222−1232.

(37) Bai, C.; Wang, Y. Study of the explosion parameters of vapor−liquid diethyl ether/air mixtures. *Journal of Loss Prevention in the Process Industries* **2015**, *38*, 139−147.

(38) Liu, X.; Zhang, Q.; Ma, Q.; Shi, Y.; Huang, Y. Limiting explosible concentration of hydrogen−oxygen−helium mixtures related to the

https://doi.org/10.1021/acsomega.3c05036
ACS Omega 2024, 9, 6381−6390

practical operational case. *Journal of Loss Prevention in the Process Industries* **2014**, *29*, 240−244.
(39) Zhang, Q.; Li, W. Ignition Characteristics for Methane-Air Mixtures atVarious Initial Temperatures. *Process Safety Progress* **2013**, *32* (1), 37−41.
(40) Zhang, Q.; Li, W.; Lin, D.-C.; He, N.; Duan, Y. Influence of nitromethane concentration on ignition energy and explosion parameters in gaseous nitromethane/air mixtures. *Journal of Hazardous Materials* **2011**, *185* (2), 756−762.
(41) Liu, X.; Huang, Y.; Wang, Y.; Zhang, Q. Critical Explosible Oxygen Concentration of Methanol-Saturated Vapor/O2/N2Mixtures at Elevated Temperatures and Pressures. *Ind. Eng. Chem. Res.* **2014**, *53* (13), 5617−5621.
(42) Bai, C.; Liu, W.; Yao, J.; Zhao, X.; Sun, B. Explosion characteristics of liquid fuels at low initial ambient pressures and temperatures. *Fuel* **2020**, *265* (3), 116951.
(43) Oran, E. S.; Chamberlain, G.; Pekalski, A. Mechanisms and occurrence of detonations in vapor cloud explosions. *Prog. Energy Combust. Sci.* **2020**, *77*, 100804.
(44) Burgoyne, J. H.; Richardson, J. F. The inflammability of oil mists. *Fuel* **1949**, *28*, 2−6.
(45) Danis, A. M.; Namer, I.; Cernansky, N. P. Droplet size and equivalence ratio effects on spark ignition of monodisperse N-heptane and methanol sprays. *Combust. Flame* **1988**, *74* (3), 285−294.
(46) Anson, D. Influence of the quality of atomization on the stability of combustion of liquid fuel sprays. *Fuel* **1953**, *32*, 39−51.
(47) Rao, K. V. L.; Lefebvre, A. H. Minimum ignition energies in flowing kerosine-air mixtures. *Combust. Flame* **1976**, *27*, 1−20.
(48) Taylor, H. D. *Flame propagation through liquid-in-air suspensions*; Department of Chemical Technology, 1957.
(49) Burgoyne, J. Mist and spray explosions. *Chem. Eng. Progress* **1957**, *3* (53), 121−124.
(50) Burgoyne, J., Ed. *The flammability of mists and sprays*, 1963.
(51) Wu, F.; Wang, H.; Yu, H.; Zang, X.; Pan, X.; Hua, M.; Jiang, J. Experimental study on the lower explosion limit and mechanism of methanol pre-mixed spray under negative pressure. *Fuel* **2022**, *321*, 124049.
(52) Jia, Y. S.; Zhang, C.; Zhang, Q.; Liang, H. M. Correlation between concentration, droplet size, turbulent intensity and explosion parameters of gas-liquid two-phase mixture. *Fire Saf. J.* **2023**, *136*, 103731.

https://doi.org/10.1021/acsomega.3c05036
ACS Omega 2024, 9, 6381−6390